ECS The Electrochemical Society
Advancing solid state & electrochemical science & technology

Electrochemistry and Morphology Studies of Aluminum Plating/Stripping in a Chloroaluminate Ionic Liquid on Porous Carbon Materials

View the article online for updates and enhancements.

Electrochemistry and Morphology Studies of Aluminum Plating/Stripping in a Chloroaluminate Ionic Liquid on Porous Carbon Materials

Mengqi Zhang,[a,*,z] **Jack S. Watson,**[a] **Robert M. Counce,**[a] **Paul C. Trulove,**[b,**]
and Thomas A. Zawodzinski Jr.[a,c,d,**]

[a]*Department of Chemical and Biomolecular Engineering, University of Tennessee, Knoxville, Tennessee 37996, USA*
[b]*Department of Chemistry, United States Naval Academy, Annapolis, Maryland 21402, USA*
[c]*Materials Science and Technology Division, Oak Ridge National Laboratory, Oak Ridge, Tennessee 37831, USA*
[d]*Department of Chemistry, King Abdulaziz University, Jeddah, Saudi Arabia*

Aluminum electrodeposition and electrodissolution in mixtures of AlCl$_3$ and 1-ethyl-3-methylimidazolium chloride on carbon paper electrodes consisting of graphitized fibers were investigated. Porous electrodes, such as carbon paper electrodes, often offer possible advantages such as higher nominal current densities and less dendrite formation, over solid planar electrodes. Cyclic voltammetry, chronoamperometry and pulse current deposition were used to investigate Al plating and stripping on this porous structure. The Al morphology on the carbon paper was probed using SEM. Composition and temperature affect the Al electrode performance through their influence on the diffusivity of ions. Therefore, control of the diffusion process during Al plating/stripping is essential.

Aluminum (Al) is the third most abundant element in the Earth's crust[1] and has three transferable electrons leading to a large theoretical specific capacity (2978 Ah/kg) when aluminum is oxidized and reduced. This makes it an excellent candidate for high energy density electrodes.[2] Al plating/stripping on/from electrodes at room temperature has been investigated AlCl$_3$/l-ethyl-3-methylimidazolium chloride (EMIC) electrolytes.[3–9] The electrochemical reaction on the Al (negative) electrode is written as:

$$\text{Negative electrode}: 4\text{Al}_2\text{Cl}_7{}^- + 3e^- \leftrightarrow \text{Al} + 7\text{AlCl}_4{}^- \qquad [1]$$
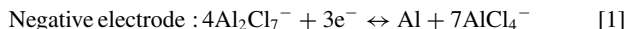
Aluminum dendrite formation has been observed, especially at high current density;[4,5] this phenomena can result in a short circuited cell.

In an effort to limit dendrite formation, three-dimensional porous carbon materials are being studied for Al plating and stripping. Based on observations of Al plating on porous carbon materials, there are several potential advantages for plating/stripping Al on porous materials over the solid planar substrates: (1) A high surface-to-volume ratio of porous materials provides the possibility of high nominal current densities. (2) By plating/stripping Al inside porous materials, formation may be controlled inside the porous structure. (3) An electrode could be designed to enhance the plating/stripping performance even further and achieve even higher current densities.

Experimental

EMIC was synthesized by using the reported procedure.[10,11] AlCl$_3$ (Fluka, >99%) was purified by sublimation in a heavy wall glass tube, as described previously.[11] The chloroaluminate melt was prepared by slowly adding EMIC onto solid AlCl$_3$ crystals. The voltammetry cell and the 3 mm diameter disk Glass Carbon (GC) electrode were purchased from Bioanalytical Systems Inc. A carbon paper electrode was prepared by cutting 2050-A carbon paper (Fuel Cell Store) to a 5 mm × 10 mm size and adhering the prepared carbon paper to one end of a copper rod (McMaster-Carr) using a silver conductive epoxy (McMaster-Carr). The surface area of the carbon paper electrode was maintained at ca. 0.5 cm^2 (5 mm × 5 mm, double sides) by using epoxy to seal the remaining electrode surface. The geometric electrode area was measured and used to calculate the current density. The reference electrode was a 1 mm diameter Al wire (Alfa Aesar, 99.999%) immersed into the molar ratio 1.5:1 AlCl$_3$: EMIC electrolyte in a glass

tube with a porous vycor tip (Bioanalytical Systems Inc.). The counter electrode was a spiral Al wire (Alfa Aesar, 99.999%). Ionic liquids were heated by a hot plate and the temperature was measured using a thermometer (Fisher Scientific Inc.). Electrochemical measurements were performed using a BioLogic SP200 potentiostat. A Hitachi TM-3000 SEM was used to observe the morphology of Al deposits on substrates.

Results and Discussion

Cyclic voltammograms (CVs) of the Al deposition and stripping processes were measured on glassy carbon (GC) and carbon paper (CP) substrates at different scanning rates. Results are shown in Figures 1 (GC) and 2 (CP).

The arrows in Figure 1 and 2 show the direction of the voltage scan. The negative current on the cyclic voltammograms is associated with the reduction reaction (Al plating process) while the positive current is associated with the oxidation reaction (Al stripping process). Based on the cyclic voltammograms shown in Figures 1 and 2, the Al plating/stripping process is a quasi-reversible reaction given the potential difference (300 mV) between reduction and oxidation peaks and the fact that this potential difference increases with the scan rate.[12] This becomes more evident in the cyclic voltammogram of Al plating on carbon paper where the current does not drop to a diffusion-controlled region at fast scan rates. The CVs in Figure 2 also are skewed with a clear linear current-voltage characteristic, indicating significant IR loss. Al plating shows only one peak but Al stripping shows two peaks, as especially evident in the 10 mV/s CV. The different peaks observed for the Al stripping process indicate a more complex electrochemical reaction mechanism upon stripping of Al. The two peaks could arise from dissolution of bulk Al and Al on the carbon surface.[4] The charge associated with the reduction and oxidation waves in Figure 2 at different scan rates were calculated. The ratio of charges is used to indicate the current efficiency. The current efficiencies are nearly 100% for 100 mV/s, 96.5% for 50 mV/s and 89.8% for 10 mV/s. This suggests that the previously observed passivation behavior due to the accumulation of Al$_2$Cl$_7{}^-$ at the electrode surface may occur at low scan rate.[4,8]

In Figure 3, we compare scans for several electrode materials to probe how the material type affects the shapes of cyclic voltammograms for Al plating and stripping. We chose a glassy carbon disk electrode, a graphite disk electrode and a carbon paper electrode for this comparison. The graphite disk electrode is assumed to have similar catalytic kinetics to carbon paper because they are both basically made of graphite. The primary difference between these two
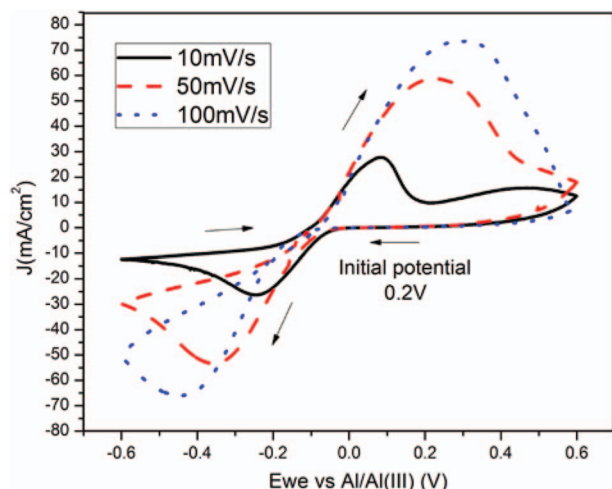
Figure 1. Cyclic voltammetry at different scanning rates on a glassy carbon disk electrode in the ionic liquid with molar ratio AlCl3:EMIC = 1.5:1

Figure 3. Cyclic voltammetry on three different electrode materials, i.e. graphite, glassy carbon and carbon paper, for Al plating/stripping at 10 mV/s.

electrodes is the configuration. One is a solid disk, and the other is a porous paper. For the disk electrodes, graphite shows better catalytic kinetics for Al plating and stripping (the slope of curve is larger than that for glassy carbon disk electrode). Furthermore, Al plating on carbon paper shows an even larger advantage over plating on the glassy carbon disk electrode. Al plating on carbon paper has a more positive onset potential than that on the graphite disk electrode but similar kinetics as the graphite disk electrode. Also, the diffusion limitation for Al plating on carbon paper is less evident than that on the graphite disk electrode. Finally, the peak current density in plating Al on carbon paper is twice the peak current density on the graphite disk electrode. This indicates that a significant difference in Al plating occurs on carbon paper, presumably arising at least in part from its porous structure.

To further investigate Al plating onto the porous carbon substrate, controlled charge chronoamperometry was used to plate Al at different overpotentials. The current transients at different overpotentials are shown in Figure 4. These current transients are acquired based on the same total amount of electric charge (0.57 mA·h). By assuming all the electric charge is utilized in the electrochemical reaction for Al deposition, the total amount of Al deposited on carbon paper should be the same for all overpotentials studied.

Figure 4 illustrates that the curve shape varies and the peak currents have different values and positions for Al deposition at different over-
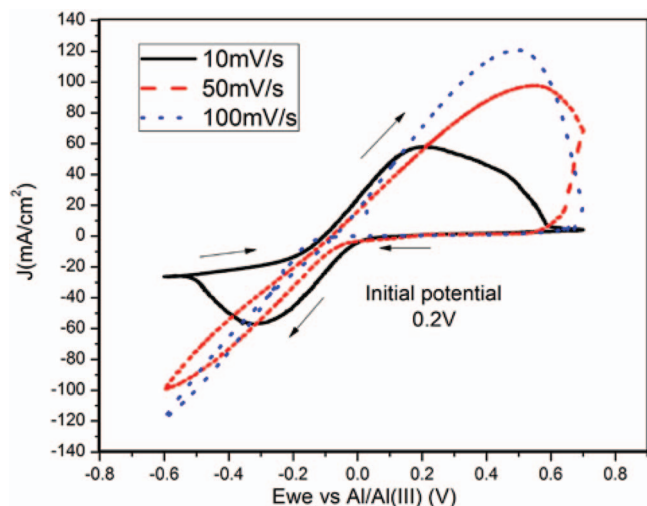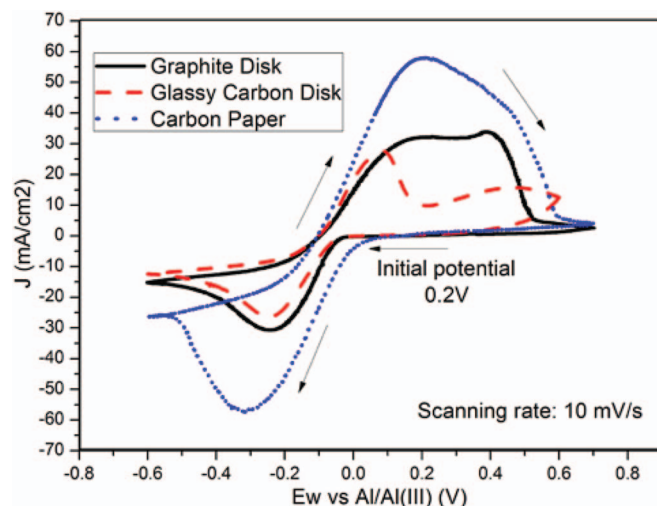
potentials. Steps to higher overpotential leads to higher current values early in the experiment. The current transients during Al plating on carbon paper are different from those observed during Al plating on disk electrodes after peak currents appear. Steady state current can be observed during Al plating on carbon paper. However, the current transients of Al plating on disk electrodes after the current peaks follow the Cottrell equation at short times.[13] This difference probably results from the shape and configuration of the porous materials. As the carbon paper is composed of graphitized fibers, the ends (tips) of these fibers on the edge of carbon paper may be active plating areas. When the ends (tips) of graphitized fibers are exposed to the electrolyte, the current at the edge of the carbon paper will gradually become an important part of the steady state current. Also, the fibers themselves may be sized and spaced to behave like individual micro-electrodes with cylindrical geometry, lending themselves to steady state behavior a long time. Similarly, nuclei and even multi-nuclear agglomerations are very small and can behave as arrays of ultramicroelectrodes with a hemispherical geometry under some conditions. SEM images are also taken to observe the morphology difference for the experiments in Figure 5.

In Figure 5 these SEM images clearly indicate that Al nuclei form at different places within the structure and with different density

Figure 2. Cyclic voltammetry at different scanning rates on a carbon paper electrode in the ionic liquid with molar ratio $AlCl_3$: EMIC = 1.5:1
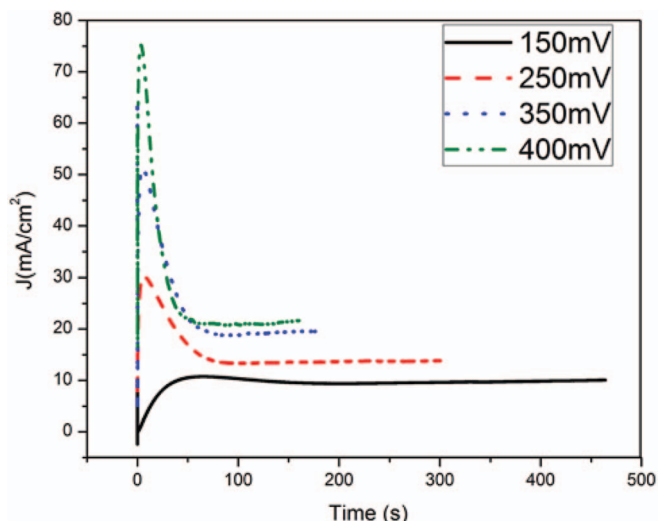

Figure 4. Current transients for Al deposition on carbon paper under different overpotentials at constant electric charge.
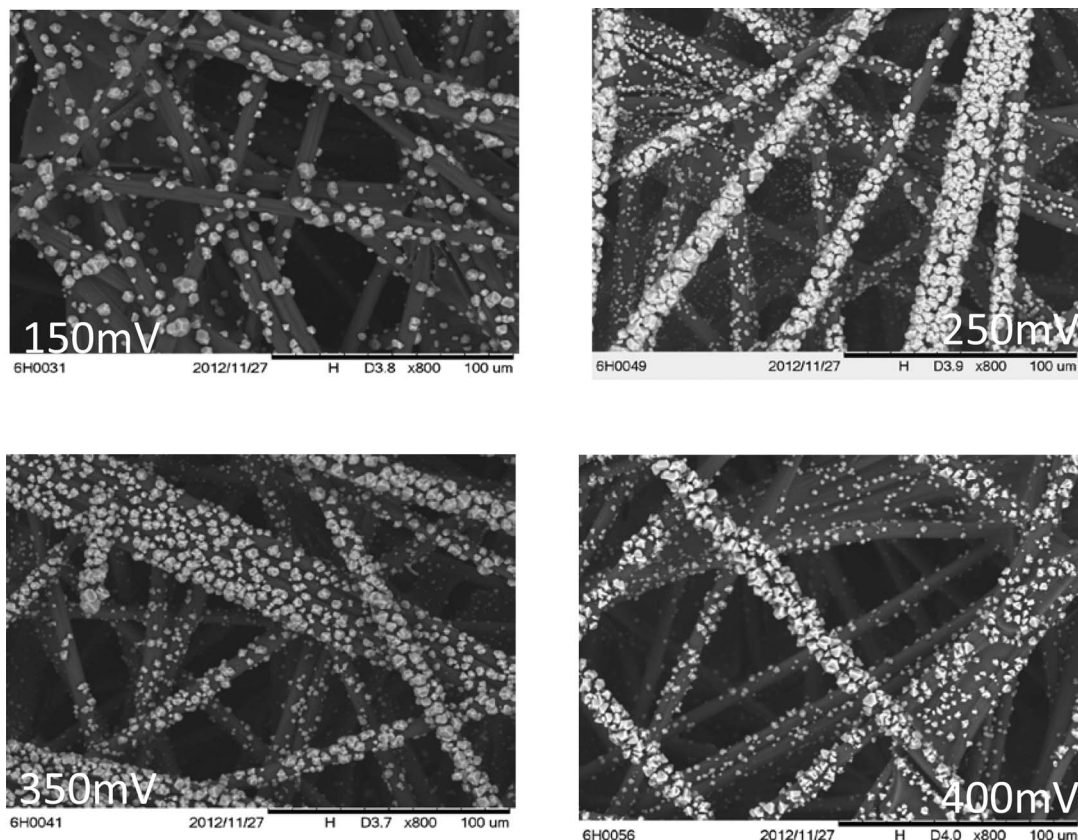
Figure 5. SEM images of Al deposition on carbon papers under different overpotential with constant electric charge.

as a function of overpotential. As noted, all of these SEM images correspond to samples with the same total amount of Al deposition by controlling electric charge. For the lower overpotential step, there are fewer nucleation sites for Al deposition, resulting in more Al deposited per site on fewer sites. With higher overpotentials, there are more nucleation sites and less Al deposited on each site. Furthermore, the sizes of Al nuclei on the inner fibers of carbon paper are smaller than those on the outer layer of carbon paper. This results from a complex

mass transfer issue. When the rate of Al nuclei growth is controlled by diffusion of ions to the outer surface of the paper, the concentration of $Al_2Cl_7^-$ on the outer layer and inner fibers of carbon paper is close to zero. Then the Al nuclei on the inner fibers of carbon paper will stop growing when the current density is controlled by the diffusion rate. Through the SEM images we also identify that the size of Al nuclei on the inner fibers of carbon paper under lower overpotential is larger than those under higher overpotential. This means that under low
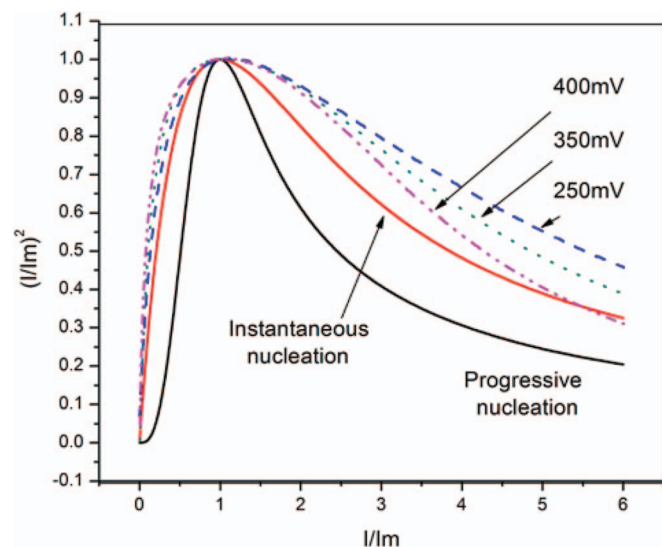

Figure 6. Comparison of dimensionless theoretical nucleation model with experimental data derived from chronoamperometric data.

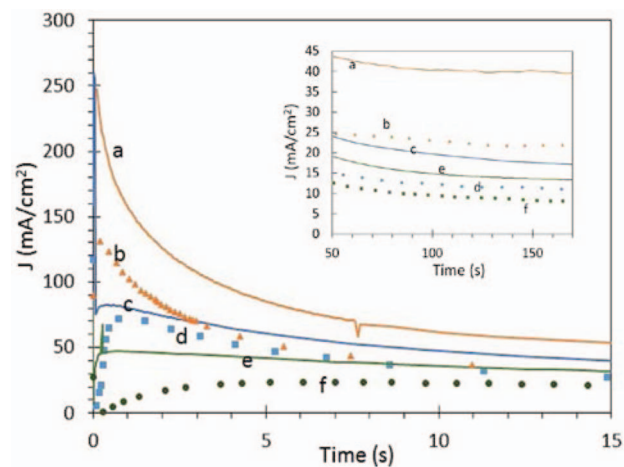**Figure 7.** Molar ratio and temperature effect on the chronoamperometry of Al plating on glassy carbon at 300 mV overpotential. (a) 2:1 molar ratio $AlCl_3$/EMIC at 70°C; (b) 1.5:1 molar ratio $AlCl_3$/EMIC at 70°C; (c) 2:1 molar ratio $AlCl_3$/EMIC at 50°C; (d) 1.5:1 molar ratio $AlCl_3$/EMIC at 50°C; (e) 2:1 molar ratio $AlCl_3$/EMIC at 30°C; (f) 1.5:1 molar ratio $AlCl_3$/EMIC at 30°C.
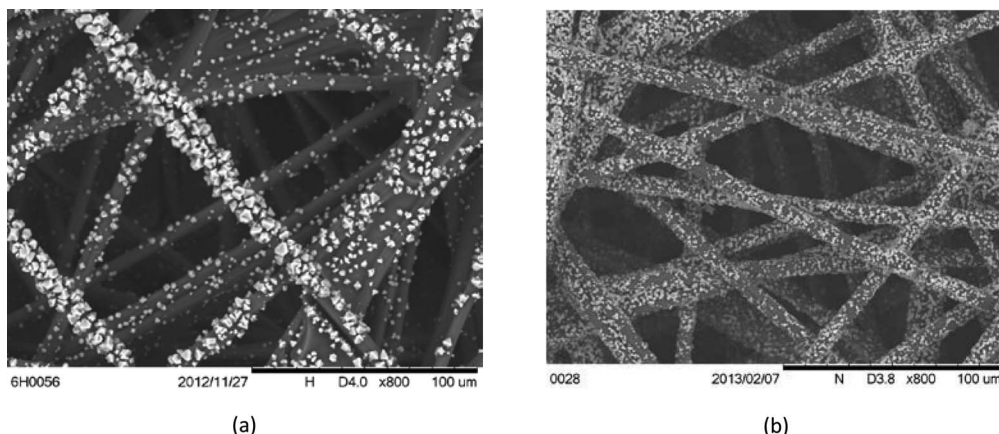
Figure 8. SEM images of Al deposition morphology under different experimental conditions. (a) controlled potential deposition at 300 mV overpotential; (b) pulse current deposition, apply 80 mA/cm^2 for 10 ms then relax for 2s.

overpotential, Al nuclei on the inner fibers of carbon paper can grow continuously for a longer time before the concentration of Al$_2$Cl$_7^-$ approaches zero. When comparing the morphology of Al nuclei under 350 mV with 400 mV overpotential, no obvious difference of Al nuclei sizes can be identified. This may result because the limiting current is reached, and the current density is only related to the diffusion rate.

As a starting point for discussion, we analyze the nucleation mechanism by the widely-used Scharifker and Hills model.[3,4] This model relates the theory of the potentiostatic current transient for 3-D multiple nucleation with diffusion controlled growth on a planar substrate. The experimental data can be compared with the theoretical prediction in Figure 6, a plot based on the following dimensionless model:

Instantaneous nucleation : $(i/i_m)^2 = 1.9542 \, (t/t_m)^{-1}$

$$\times \{1 - exp\,[-1.2564 \, (t/t_m)]\}^2$$

$$[2]$$

Progressive nucleation : $(i/i_m)^2 = 1.2254 \, (t/t_m)^{-1}$

$$\times \{1 - exp\,[-2.3367 \, (t/t_m)]\}^2$$

$$[3]$$

where i$_m$ represents the peak current density; t$_m$ means the time when the peak current occur.[13]

The Scharifker and Hills model posits that the current transient consists of two parts. The current transient first rises to a current peak and then decreases following the Cottrell equation.[13] The current peaks are considered to reflect the summed current from each nuclei and the current drop-off results from the overlapping of diffusion layers as the nuclei form and particles grow. As the plot in Figure 6 shows, the dimensionless description of experimental data from current transients do not vary strongly with the overpotential. We conclude that the overpotential may not affect the nucleation mechanism. However, the experimentally observed dimensionless data deviates from the Scharifker and Hills model prediction, especially after the current peaks. We suggest that this is because it takes longer for the overlap of diffusion layers of the Al nuclei on the porous materials because of the three-dimensional nature of the substrate. Clearly, the assumptions of the Scharifker and Hills model are different from the current situation where porous materials are used as substrates. Their model assumed that the deposition takes place on a planar substrate with semi-finite linear diffusion. However, the carbon paper consists of graphitized fibers (diameter ca.7–8 um) and the cylindrical/ spherical diffusion and edge effects in the diffusion process are not taken into consideration in the Scharifker and Hills model.

The molar ratio of AlCl$_3$ and EMIC will affect the concentration of Al$_2$Cl$_7^-$ and AlCl$_4^-$ in the chloroaluminate melts. The Al$_2$Cl$_7^-$ concentration increases and reaches a maximum when the molar ra-

tio of AlCl$_3$ and EMIC approaches 2. In this composition regime, the melt viscosity is also at a minimum. These factors lend themselves to high diffusional flux of Al$_2$Cl$_7^-$ to the electrode surface. Higher temperature will also result in a faster kinetic process and high diffusivity of Al$_2$Cl$_7^-$ and AlCl$_4^-$. Increases of these two parameters can lead to higher current densities for Al plating and stripping. The chronoamperometry shown in Figure 7 illustrates how molar ratio and temperature enhance the current density of plating Al.

Al plating involves a nucleation and Al particle growth. The Al growth is considered to be a diffusion-controlled process.[2,3] Initially each Al nucleus has a hemi-spherical diffusion zone. When charge-transfer is fast (large overpotential), these diffusion zones merge together because the concentration of ions near the electrode surface is depleted. Finally a semi-infinite linear diffusion characteristic is achieved when the substrate behaves as if it has a planar configuration. To test the possibility of a diffusion effect on plating Al on the inner fibers of carbon paper, pulse current deposition is applied. The following SEM images in Figure 8 show the difference of Al morphology between controlled constant potential and pulsed currents.

Al plating on carbon paper using the pulse current deposition technique allows more Al to be plated on the inner fibers of carbon paper. By applying the current density on the carbon paper at a certain frequency, the diffusion layers of each Al nucleus will grow and shrink following pulsed current and do not have enough time to overlap with each other. During the relaxation time, ions such as Al$_2$Cl$_7^-$, will be resupplied to the fiber surfaces not only on the outer carbon paper surfaces, but also inside carbon paper. This indicates that the Al nuclei can continue growing on the fibers inside the carbon paper.

Conclusion

Al can be plated and stripped on a carbon paper electrode. The porous structure of carbon paper leads to different behavior, relative to planar electrodes, for cyclic voltammograms, current transients at controlled potentials and Al morphology. The porous materials are promising substrates to enhance the performance of the Al electrode on current density. The overpotential for Al deposition on carbon paper is lower than that on glassy carbon. Current transients for Al deposition on a planar substrate and the fibrous, porous substrate are also different. A test of the Scharifker and Hills model clearly shows that it is not suitable to capture the Al nucleation and growth phenomena on carbon paper. Edge effects and cylindrical diffusion should be considered to build a new nucleation model for porous substrates. Higher temperatures and higher AlCl$_3$ molar compositions improve the performance of Al plating by raising the nucleation rate and diffusion rate of ions. The diffusion of ions to the fibers inside carbon paper is an important process determining the locus and site density for Al plating as a function of depth into the carbon paper. Pulsed

plating allows depletion effects arising from insufficient diffusion rates into the paper to relax and leads to a more uniform distribution of Al particles. These results provide a preliminary indication that a porous electrode can be tailored to provide a good option for Al plating on carbon paper.

References

1. F. W. Clarke and H. S. Washington, *The Composition of the Earth's Crust*, (1924).
2. Q. Li and N. J. Bjerrum, *Journal of power sources*, **110**, 1 (2002).
3. R. T. Carlin, W. Crawford, and M. Bersch, *Journal of Electrochemical Society*, **139**, 2720 (1992).
4. T. Jiang, M. J. Chollier Brym, G. Dubé, a. Lasia, and G. M. Brisard, *Surface and Coatings Technology*, **201**, 1 (2006).
5. D. Pradhan, D. Mantha, and R. G. Reddy, *Electrochimica Acta*, **54**, 6661 (2009).
6. P. Lai and M. Skyllas-Kazacos, *Journal of Electroanalytical Chemistry*, **248**, 431 (1988).
7. S. Schaltin, M. Ganapathi, K. Binnemans, and J. Fransaer, *Journal of The Electrochemical Society*, **158**, D634 (2011).
8. J. Auborn and Y. Barberio, *Journal of the Electrochemical Society*, **132**, 598 (1985).
9. F. Endres, M. Bukowski, R. Hempelmann, and H. Natter, *Angewandte Chemie (International ed. in English)*, **42**, 3428 (2003).
10. J. S. Wilkes, J. A. Levisky, R. A. Wilson, and C. L. Hussey, *Inorganic Chemistry*, **21**, 1263 (1982).
11. P. C. Trulove, The Chemistry of Proton in Ambient-temperature Chloroaluminate Molten Salts, Thesis, State of University of New York, Buffalo, 25-44 (1992).
12. A. J. Bard and L. R. Faulkner, *Electrochemical Methods: Fundamentals and Applications, 2nd ed.*, John Wiley & Sons, Inc, New York, USA, (2001).
13. B. Scharifker and G. Hills, *Electrochimica Acta*, **28**, 879 (1982).